

Optimization Schemes for Efficient Multiple Exciton Generation and Extraction in Colloidal Quantum Dots

Fikeraddis A. Damtie,^{1, a)} Khadga J. Karki,^{2, b)} Tõnu Pullerits,^{2, c)} and Andreas Wacker^{1, d)}

¹⁾ *Mathematical Physics and NanoLund, Lund University, Box 118, 22100 Lund, Sweden.*

²⁾ *Chemical Physics and NanoLund, Lund University, Box 124, 22100 Lund, Sweden.*

(Dated: 25. July 2016; accepted by The Journal of Chemical Physics, 2016)

Multiple exciton generation is a process in which more than one electron hole pair is generated per absorbed photon. It allows us to increase the efficiency of solar energy harvesting. Experimental studies have shown the multiple exciton generation yield of 1.2 in isolated colloidal quantum dots. However real photoelectric devices require the extraction of electron hole pairs to electric contacts. We provide a systematic study of the corresponding quantum coherent processes including extraction and injection and show that a proper design of extraction and injection rates enhances the yield significantly up to values around 1.6.

PACS numbers: 71.35.-y; 78.67.-n; 88.40.hj

Keywords: Multiple exciton generation; Quantum dots; Optical excitation; Solar cells

I. INTRODUCTION

In recent years colloidal semiconductor quantum dots (QDs) have shown promise as photovoltaic material. Quantum confinement in QDs allows convenient tuning of the absorption over the whole solar spectrum leading to the so called "rainbow" solar cells¹. Most promising, however, is the process known as multiple exciton generation (MEG)^{2–10}. MEG is the generation of more than one electron hole pair with energies close to the bandgap upon the absorption of a single high energy photon^{5,11–14}. The process is a result of Coulomb electron-electron interaction (in the form of an inverse Auger process), which is more significant in QDs than in bulk structures due to the forced overlap of electronic wavefunctions¹⁵. In addition, confinement leads to the absence of conservation of momentum, modified carrier-cooling rates and reduced dielectric screening, all of which account for enhanced MEG in QDs^{15,16}. Besides this basic understanding, a detailed microscopic description of MEG in QDs is needed for an efficient design and optimization of QD solar cells. Since the first demonstration of efficient MEG in PbSe QDs by Schaller and Klimov in 2004⁵, a significant attention has been paid towards the study of QD based systems for efficient MEG. Several groups have been studying MEG efficiency in colloidal semiconductor QDs where they showed a production of multiple electron hole pairs upon absorption of a single photon^{12,16–18}. Lead Chalcogenide QDs (PbS and PbSe), Cadmium Chalcogenide QDs, Indium based QDs (InAs and InP) and Silicon QDs are some of the intensively studied QD systems for exploring the efficiency of

MEG^{2,19–24}. MEG is commonly measured by ultrafast transient absorption spectroscopy²⁵, which allows one to capture the rapid processes of bi-exciton formation and Auger recombinations on the ps time scale²⁶. These processes occur at much faster timescale as compared to the lifetimes of single excitons (ns time scale)²⁷. Recently, we have established a model to study this time-dependence²⁸, which describes bi-exciton formation in good agreement with time-resolved measurements²⁰.

In a real solar cell generating current, the extraction and injection of charge carriers is of central relevance^{29,30}. Efficient MEG combined with the extraction of electron hole pairs has been demonstrated by several groups in the past. An increased peak external quantum efficiency due to MEG was reported for PbSe³¹ and PbS⁴ QDs. Similarly, increases exceeding 120% have been reported in PbTe QDs⁷ and PbSe nanorods³². Quantitatively, the injection and extraction rates of carriers between the dot and its environment can depend highly on material parameters such as the band alignment and the geometry of the physical realization³³. In this work, we explore the parameter regimes for efficient extraction of charge carriers produced with the MEG scheme. The aim is to guide the design of optimal couplings between the QDs and the relevant donor and acceptor reservoirs.

For the exciton generation, we consider a short laser pulse. This is guided by corresponding optical measurements. The double exciton generation is due to the Coulomb electron-electron interaction, which we take into account by diagonalising the QD system with full inter-particle interaction as described in Ref. 28. Ideally, in the absence of coupling to the outside environment, one expects that amplitudes in the two states can oscillate indefinitely in a way similar to the Rabi oscillation in isolated two level system^{14,17}. However, in reality relaxation and dephasing limit such coherent behavior. This is described by a Lindblad master equation here. As in Ref. 28, we take into account pure dephasing, relaxation

^{a)} Electronic mail: Fikeraddis.Damtie@teorfys.lu.se

^{b)} Electronic mail: Khadga.Karki@chemphys.lu.se

^{c)} Electronic mail: Tõnu.Pullerits@chemphys.lu.se

^{d)} Electronic mail: Andreas.Wacker@fysik.lu.se

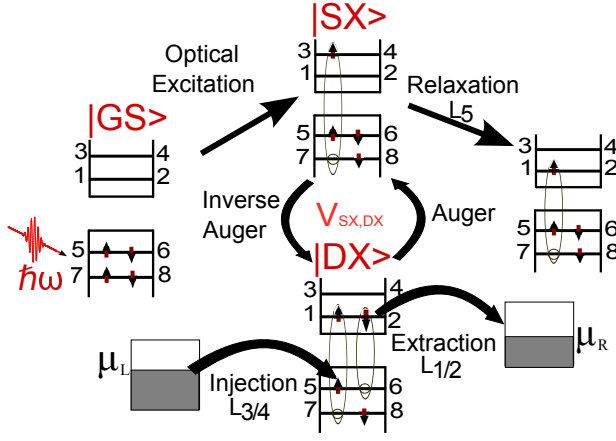


FIG. 1. The various physical processes considered in the study namely, optical excitation by a resonant pulse, Auger recombination, extraction and injection to and from a reservoir with chemical potential μ_R and μ_L respectively. In addition we consider relaxation, which is competing with the Auger process.

within the bands and recombination between the bands, which is typically the slowest process. In addition, we consider the extraction and injection of charge carriers to and from the QD. This allows for a more realistic description of the yield for the device, which here is defined as the number of extracted electrons per absorbed photon.

The observable yield depends on two issues: Firstly, the double excitons must be produced and secondly their presence needs to be detected. As the exciton generation and their subsequent evolution is a coherent process, any detection may substantially modify the behavior. Therefore a careful definition of the yield based on the experimental setup is important³⁴. For isolated dots, the yield was measured by the bleach signal of the exciton absorption on a timescale of tens of ps after the excitation²⁰. This average exciton occupation probability corresponds to the recombination of excitons, which was used to define the yield in our earlier study²⁸. In this work we consider a photoelectric device by including the injection and extraction of charges. This allows for a more practical definition of the yield based on the number of the extracted electron hole pairs. Compared to our earlier study, we find higher yields, as the extraction reduces the probability for the double exciton to return back to the single exciton via Auger recombination.³⁵ This clearly demonstrates the relevance of properly designed contacts for the injection and the extraction of the charges and this work contributes to their optimization.

II. MODEL

Figure 1 sketches our model for the QD and the main physical processes considered in the study which are out-

lined in detail below. An optical excitation by a resonant pulse creates the single exciton state $|SX\rangle$ from the ground state $|GS\rangle$. The single exciton state is transferred to the double exciton state $|DX\rangle$ by an inverse Auger process. However, electron relaxation by other processes, such as phonon scattering, are competing process here. Once the double exciton is formed, it is desirable to extract the electrons from the levels 1 and 2 by an efficient mechanism before it returns back to the single exciton state via an Auger process. In the many-particle description applied here the Auger process and its inverse appear as the coherent oscillation between the states $|SX\rangle$ and $|DX\rangle$ due to the coupling by the Coulomb matrix element $V_{SX,DX}$, see Ref. 28 and 17

Many particle states

The total Hamiltonian for the system can be divided into two main parts, the time independent Hamiltonian \hat{H}_0 of the dot, which fully includes the Coulomb interaction \hat{H}_{ee} between the electrons, and the time dependent interaction with the oscillating electric field, $\hat{H}_I(t)$.

$$\hat{H}_{\text{eff}}(t) = \underbrace{\sum_i E_i \hat{a}_i^\dagger \hat{a}_i}_{\hat{H}_0} + \hat{H}_{ee} + \hat{H}_I(t) \quad (1)$$

All the operators are expressed in occupation number representation with the creation/annihilation operators $\hat{a}_i^\dagger/\hat{a}_i$ for electrons in the single particle levels i having energy E_i . The many body states used in our calculations are obtained by exact diagonalization of \hat{H}_0 . We use parameters corresponding to a 4 nm PbS QD following Ref. 28, where further details can be found.

Equation of motion for the density matrix

The QD is excited by an optical pulse, which we describe in dipole approximation as

$$\hat{H}_I(t) = \underbrace{eE_0 e^{-t^2/\tau^2} \sin(\omega t)}_{E(t)} \sum_{mn} z_{mn} \hat{a}_m^\dagger \hat{a}_n \quad (2)$$

Throughout this study we use $\tau = 150$ fs, $eE_0 z_{37} \approx -0.317$ meV, and $\hbar\omega \approx 4.25$ eV, which corresponds to a 0.035π pulse in resonance with the $7 \rightarrow 3$ (and $8 \rightarrow 4$) transition taking into account the Coulomb interaction in the ground state. (Thus, slightly different values of $\hbar\omega$ will be used in calculations with a modified Coulomb strength below.) The time evolution of the reduced density operator for the system is evaluated by the Lindblad

equation³⁶

$$\hbar \frac{d}{dt} \hat{\rho}_S(t) = i[\hat{\rho}_S(t), \hat{H}_{\text{eff}}(t)] + \sum_{j=1}^{N_{\text{jump}}} \Gamma_j \left[\hat{L}_j \hat{\rho}_S \hat{L}_j^\dagger - \frac{1}{2} (\hat{L}_j^\dagger \hat{L}_j \hat{\rho}_S + \hat{\rho}_S \hat{L}_j^\dagger \hat{L}_j) \right]. \quad (3)$$

Here, the jump operators \hat{L}_j describe different dissipation processes (with rate Γ_j/\hbar), which are restoring the ground state for sufficiently long times after the excitation.

Dissipative processes considered

We use the convention that carriers with up spins \uparrow occupy odd numbered and those with down spin \downarrow occupy even numbered single particle levels in all the definitions below. The following dissipative processes are taken into account in the model cf. Fig. 1: Extraction from the conduction band edge

$$\hat{L}_1 = \hat{a}_{1\uparrow} \text{ and } \hat{L}_2 = \hat{a}_{2\downarrow} \quad \text{with strength } \Gamma_{\text{Ext}}$$

Injection into the valence band edge

$$\hat{L}_3 = \hat{a}_{5\uparrow}^\dagger \text{ and } \hat{L}_4 = \hat{a}_{6\downarrow}^\dagger \quad \text{with strength } \Gamma_{\text{Inj}}$$

Relaxation in the conduction band

$$\hat{L}_5 = \hat{a}_{1\uparrow}^\dagger \hat{a}_{3\uparrow} + \hat{a}_{2\downarrow}^\dagger \hat{a}_{4\downarrow} \quad \text{with strength } \Gamma_{\text{Rel}}$$

Relaxation in the valence band

$$\hat{L}_6 = \hat{a}_{7\uparrow}^\dagger \hat{a}_{5\uparrow} + \hat{a}_{4\downarrow}^\dagger \hat{a}_{8\downarrow} \quad \text{with strength } \Gamma_{\text{Rel}}$$

Recombination across the band gap

$$\hat{L}_7 = \hat{a}_{5\uparrow}^\dagger \hat{a}_{1\uparrow} + \hat{a}_{6\downarrow}^\dagger \hat{a}_{2\downarrow} \quad \text{with strength } \Gamma_{\text{Rec}}$$

Dephasing of all states

$$\begin{aligned} \hat{L}_8 &= \hat{a}_{1\uparrow}^\dagger \hat{a}_{1\uparrow} + \hat{a}_{2\downarrow}^\dagger \hat{a}_{2\downarrow} \\ \hat{L}_9 &= \hat{a}_{3\uparrow}^\dagger \hat{a}_{3\uparrow} + \hat{a}_{4\downarrow}^\dagger \hat{a}_{4\downarrow} \\ \hat{L}_{10} &= \hat{a}_{5\uparrow}^\dagger \hat{a}_{5\uparrow} + \hat{a}_{6\downarrow}^\dagger \hat{a}_{6\downarrow} \\ \hat{L}_{11} &= \hat{a}_{7\uparrow}^\dagger \hat{a}_{7\uparrow} + \hat{a}_{8\downarrow}^\dagger \hat{a}_{8\downarrow} \end{aligned} \quad \text{with strength } \Gamma_{\text{Deph}}$$

The jump operators are defined in such a way that they all conserve the total spin if the particle number is conserved. The different decoherence mechanisms, which are phenomenologically described in Eq. (3), can be associated to all forms of intrinsic scattering mechanisms other than electron-electron scattering, which has already been included in the effective Hamiltonian.

In all the simulations, the dephasing rate $\Gamma_{\text{Deph}} = 6$ meV which corresponds to $\tau_{\text{Deph}} = 0.69$ ps is applied. As the recombination is typically the slowest time scale (unless for very weak coupling to the reservoir not considered here), we neglect this process in our study and

set $\Gamma_{\text{Rec}} = 0$, which corresponds to $\tau_{\text{Rec}} = \infty$ throughout this work. (Test calculations showed only very small changes of about 5% for $\Gamma_{\text{Rec}} = 0.1$ meV with the corresponding rate in time units of $\tau_{\text{Rec}} = 41.3$ ps, which is fairly large compared to the typical recombination rates in semiconductor dots.) The extraction and injection processes require certain energy ranges for the incoming and outgoing particles. If the jump operator corresponds to adding a particle (injection), the initial system with particle number N has an energy $E(N)$. The incoming particle should have an energy such that it enters the valence band levels (5 or 6) depending on the spin. After the jump, the system will have $N + 1$ particles with energy $E(N + 1)$. The injecting contact for such a photovoltaic system has its electrochemical potential a small margin Δ above the highest occupied level in the valence band, as depicted in Fig. 1. Thus, electrons can only enter if $(E(N + 1) - E(N)) \leq (E_g(4) - E_g(3)) + \Delta$. Here, $E_g(N)$ denotes the ground state for N particles as obtained from the diagonalization of \hat{H}_0 . Temperature broadening is neglected for simplicity. Similarly, the jumps associated with the removal of a particle (extraction), require empty states in the corresponding reservoir, which are available above its electrochemical potential. This is a small margin Δ below the lowest level in the conduction band and provides the required energy $(E(N) - E(N - 1)) \geq (E_g(5) - E_g(4)) - \Delta$ for the removal of an electron from an N -electron state. In all our calculations, we use $\Delta = 0.2$ eV.

III. RESULTS AND DISCUSSION

The focus of our work is to determine parameter regimes in which the total number of extraction of charged particles from the band edges is optimal per single absorbed photon. Here, we calculate the average number of particles extracted from the conduction band after the pulse excitation. The extraction rate is

$$\text{Ext}(t) = \sum_{i=1,2} \Gamma_{\text{Ext}} \text{Tr}\{\hat{L}_i \hat{\rho} \hat{L}_i^\dagger\} \quad (4)$$

so that the average number of extracted electron is given by

$$\text{Number of extraction} = \int_{-\infty}^{\infty} dt \text{Ext}(t). \quad (5)$$

This quantity is plotted in Figure 2a as a function of the extraction rate, Γ_{Ext} , for electrons from the conduction band and the injection rate, Γ_{Inj} , for electrons into the valence band by appropriately designed contacts. As expected, we find that the number of extractions increases with increasing reservoir coupling for either contact, as competing relaxation processes become less relevant. Note that the number of injections, as obtained by summing over jump processes 3 and 4, equals the number of extractions, as the system returns into the ground

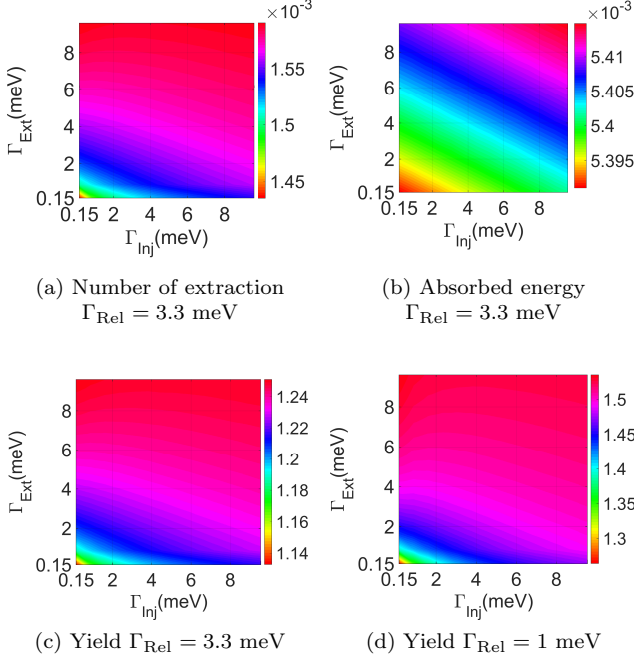


FIG. 2. Number of extractions (a) and absorbed energy (b) for different reservoir coupling strengths. The ratio between these numbers determines the yield in panel (c). Panel (d) shows the yield for a reduced relaxation rate.

state with 4 electrons occupying the levels 5–8 for large times. Thus, the number of extractions and the number of injections constitute the same measure for the current flow through the dot.

In order to determine the yield, we need the number of absorbed photons for comparison. Therefore we consider the energy balance for the interaction with the light field³⁷

$$P(t) = \frac{d}{dt} \langle \hat{H}_{\text{eff}}(t) \rangle = \left\langle \frac{\partial \hat{H}_I(t)}{\partial t} \right\rangle = e \langle \hat{z} \rangle \dot{E}(t) \quad (6)$$

such that the total energy transferred from the light pulse to the dot is

$$\text{Absorbed Energy} = \int_{-\infty}^t dt P(t). \quad (7)$$

This quantity is displayed in Figure 2b and is only changing slightly with the contact couplings. Our main point of interest is the yield, i.e., the ratio between the number of extraction and the absorbed energy per the incoming photon energy.:

$$\text{Yield} = \frac{\text{Number of extraction}}{\text{Absorbed Energy}} \times \hbar \omega_{\text{pulse}}. \quad (8)$$

Figure 2c shows that the yield varies between $\approx 1.13 - 1.25$ for different injection and extraction rates for $\Gamma_{\text{Rel}} = 3.3$ meV. It can be seen that higher rates of extraction and injection in general result in a higher yield. This is

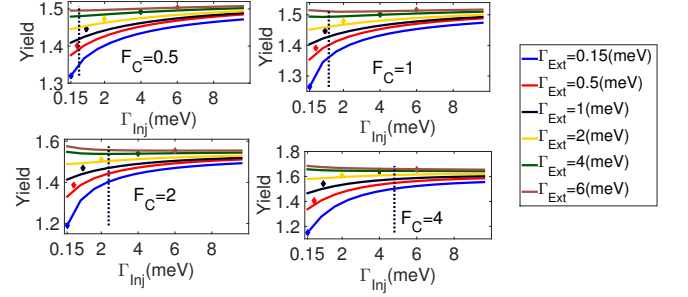


FIG. 3. Yield as a function of the injection rates for different rates of extraction. Different strengths for the Auger coupling rate are applied in each panel. The vertical line denotes $\Gamma_{\text{Inj}} = 2V_{1263}^{ee}$ and the diamonds refer to the points $\Gamma_{\text{Inj}} = \Gamma_{\text{Ext}}$. The relaxation rate $\Gamma_{\text{Rel}} = 1$ meV is used here.

due to the fact that the double exciton is efficiently extracted before it goes back to the single exciton state via the inverse Auger recombination. Comparing the increment in the yield as a function of the extraction and injection rate, it can be seen that the yield increases faster as a function of extraction and saturates more quickly than upon varying the injection rate. The reason for this behavior is that the extraction involves the electrons in the conduction band, which are created as a result of the Coulomb electron-electron interaction. On the other hand, the injection rate involves the electrons in the valence band, which increases the yield only if the extraction rate is small. This increase is due to the fact that injection into the level 6 hinders the Auger process converting the $|DX\rangle$ state back to the $|SX\rangle$ state, see Fig. 1. This provides a relevant termination process for the coherent oscillations between the $|DX\rangle$ and $|SX\rangle$ state, if the extraction rate is small. Figure 2d shows similar results but with a smaller relaxation rate. It can be seen that the overall yield increases for the ranges shown. Low relaxation rate indeed results in a larger chance for the inverse Auger process to occur before the single exciton relaxes to some other low energy state. As a result, the creation and extraction of the double exciton is enhanced for reduced relaxation.

Since MEG involves a competing process between the Auger kinetics and the relaxation, it is of interest, to study how these relate to each other quantitatively. The inverse Auger process is dominated by the Coulomb matrix element $V_{1263}^{ee} = -0.6$ meV. In order to quantify its role, we now modify this matrix element (as well as the one with spins exchanged and the adjoint ones) by multiplying them with a factor F_C .

Fig. 3 shows the yield as a function of injection rate for the different strengths of the Coulomb coupling for the Auger terms. The energy splitting $|E_{SX} - E_{DX}| \approx 2|V_{1263}^{ee}|$ in each simulation is indicated by a dashed vertical line for better comparison with respect to the extraction and injection rates. In addition, the extraction rates for each line is indicated by a diamond with the corre-

sponding colors for each extraction rate. As expected, the yield increases with increasing either the extraction or the Auger coupling for all cases. Here, we find that in the case where the Auger Coulomb coupling is dominant over the extraction rate, $2|V_{1263}^{ee}| > \Gamma_{\text{Ext}}$, the yield is small as the coherent oscillation between the $|SX\rangle$ and $|DX\rangle$ states is only damped by the relaxation processes. However, the $|DX\rangle$ state can be conserved by the injection of an electron into the valence band and thus we find a significant increase of yield with Γ_{Inj} under these conditions, which levels off for $\Gamma_{\text{Inj}} \gg 2|V_{1263}^{ee}|$. On the other hand, for $\Gamma_{\text{Ext}} > 2|V_{1263}^{ee}|$ where extraction is dominant, the variation of the yield as a function of the injection rate is small. In this case, the extraction is sufficient to guarantee high yield.

IV. CONCLUSION

In this work, we have examined the conditions for optimal MEG by impact ionization upon optical excitation by high energy photons. We have focused on the extraction and injection mechanisms of charge carriers, which are key ingredients in a realistic device. We have shown that an optimal yield can be achieved by an efficient extraction mechanism, which exceeds the Coulomb coupling matrix element for the inverse Auger process. Furthermore, relaxation should be kept slow. For small extraction rates compared to the Coulomb matrix element between the single exciton and double exciton states, an increase in the injection rate improves the yield by altering the oscillation between $|SX\rangle$ and $|DX\rangle$. More importantly, our work shows that the MEG yield in photovoltaic devices can be higher than in QDs dispersed in solution that have no contacts for the extraction of the charges.

V. ACKNOWLEDGMENTS

We acknowledge the Knut and Alice Wallenberg foundation (KAW), NanoLund as well as the Swedish Research Council (VR) for financial support.

VI. REFERENCES

- ¹A. Kongkanand, K. Tvrđy, K. T. M. Kuno, and P. V. Kamat, *J. Am. Chem. Soc.* **130**, 4007 (2008).
- ²M. C. Beard, K. P. Knutsen, P. Yu, J. M. Luther, Q. Song, W. K. Metzger, R. J. Ellingson, and A. J. Nozik, *Nano Letters* **7**, 2506 (2007).
- ³A. Nozik, *Physica E* **14**, 115 (2002).
- ⁴J. B. Sambur, T. Novet, and B. A. Parkinson, *Science* **330**, 63 (2010).
- ⁵R. D. Schaller and V. I. Klimov, *Phys. Rev. Lett.* **92**, 186601 (2004).
- ⁶X. Lan, S. Masala, and E. H. Sargent, *Nat. Mater.* **13**, 233 (2014).
- ⁷M. L. Böhm, T. C. Jellicoe, M. Tabachnyk, N. J. L. K. Davis, F. Wisnivesky-Rocca-Rivarola, C. Ducati, B. Ehrler, A. A. Bakulin, and N. C. Greenham, *Nano Letters* **15**, 7987 (2015).
- ⁸P. V. Kamat, *J. Phys. Chem. Lett.* **4**, 908 (2013).
- ⁹K. Zheng, K. Karki, K. Židek, and T. Pullerits, *Nano Res.* **8**, 2125 (2015).
- ¹⁰M. Abdellah, R. Marschan, K. Židek, M. E. Messing, A. Abdelwahab, P. Chábera, K. Zheng, and T. Pullerits, *J. Phys. Chem. C* **118**, 25802 (2014).
- ¹¹K. J. Karki, J. R. Widom, J. Seibt, I. Moody, M. C. Lonergan, T. Pullerits, and A. H. Marcus, *Nat. Commun.* **5**, 5869 (2014).
- ¹²M. C. Beard, *J. Phys. Chem. Lett.* **2**, 1282 (2011).
- ¹³A. J. Nozik, *Chem. Phys. Lett.* **457**, 3 (2008).
- ¹⁴A. Shabaev, A. L. Efros, and A. J. Nozik, *Nano Letters* **6**, 2856 (2006).
- ¹⁵V. I. Klimov, *Annu. Rev. Phys. Chem.* **58**, 635 (2007).
- ¹⁶M. C. Beard, A. G. Midgett, M. C. Hanna, J. M. Luther, B. K. Hughes, and A. J. Nozik, *Nano Letters* **10**, 3019 (2010).
- ¹⁷R. J. Ellingson, M. C. Beard, J. C. Johnson, P. Yu, O. I. Micic, A. J. Nozik, A. Shabaev, and A. L. Efros, *Nano Letters* **5**, 865 (2005).
- ¹⁸M. C. Beard, J. M. Luther, O. E. Semonin, and A. J. Nozik, *Acc. Chem. Res.* **46**, 1252 (2013).
- ¹⁹D. Gachet, A. Avidan, I. Pinkas, and D. Oron, *Nano Letters* **10**, 164 (2010).
- ²⁰K. J. Karki, F. Ma, K. Zheng, K. Židek, A. Mousa, M. A. Abdellah, M. E. Messing, L. R. Wallenberg, A. Yartsev, and T. Pullerits, *Sci. Rep.* **3**, 2287 (2013).
- ²¹J. J. H. Pijpers, E. Hendry, M. T. W. Milder, R. Fanciulli, J. Savolainen, J. L. Herek, D. Vanmaekelbergh, S. Ruhman, D. Mocatta, D. Oron, A. Aharoni, U. Banin, and M. Bonn, *J. Phys. Chem. C* **111**, 4146 (2007).
- ²²R. D. Schaller, M. A. Petruska, and V. I. Klimov, *Appl. Phys. Lett.* **87**, 253102 (2005).
- ²³S. K. Stubbs, S. J. O. Hardman, D. M. Graham, B. F. Spencer, W. R. Flavell, P. Glarvey, O. Masala, N. L. Pickett, and D. J. Binks, *Phys. Rev. B* **81**, 081303 (2010).
- ²⁴F. W. Wise, *Acc. Chem. Res.* **33**, 773 (2000).
- ²⁵F. Träger, *Springer handbook of lasers and optics* (Springer Science & Business Media, 2007).
- ²⁶V. I. Klimov, A. A. Mikhailovsky, D. W. McBranch, C. A. Leatherdale, and M. G. Bawendi, *Science* **287**, 1011 (2000).
- ²⁷S. A. Crooker, T. Barrick, J. A. Hollingsworth, and V. I. Klimov, *Appl. Phys. Lett.* **82**, 2793 (2003).
- ²⁸F. A. Damtie and A. Wacker, *J. Phys.:Conf. Ser.* **696**, 012012 (2016).
- ²⁹K. Židek, K. Zheng, M. Abdellah, N. Lenngren, P. Chábera, and T. Pullerits, *Nano Letters* **12**, 6393 (2012).
- ³⁰K. Zheng, K. Židek, M. Abdellah, W. Zhang, P. Chábera, N. Lenngren, A. Yartsev, and T. Pullerits, *J. Phys. Chem. C* **118**, 18462 (2014).
- ³¹O. E. Semonin, J. M. Luther, S. Choi, H.-Y. Chen, J. Gao, A. J. Nozik, and M. C. Beard, *Science* **334**, 1530 (2011).
- ³²N. J. Davis, M. L. Böhm, M. Tabachnyk, F. Wisnivesky-Rocca-Rivarola, T. C. Jellicoe, C. Ducati, B. Ehrler, and N. C. Greenham, *Nat. Commun.* **6**, 8259 (2015).
- ³³T. Hansen, K. Židek, K. Zheng, M. Abdellah, P. Chábera, P. Persson, and T. Pullerits, *J. Phys. Chem. Lett.* **5**, 1157 (2014).
- ³⁴D. J. Binks, *Phys. Chem. Chem. Phys.* **13**, 12693 (2011).
- ³⁵The double exciton formation and the Auger recombination are parts of the same coherent process generated by the Coulomb coupling between these states. While such terms help in the discussion and qualitative understanding of results, one cannot not separate these processes entirely.
- ³⁶G. Lindblad, *Comm. Math. Phys.* **48**, 119 (1976).
- ³⁷S. Mukamel, *Principles of nonlinear optical spectroscopy*, Vol. 29 (Oxford University Press New York, 1995).